

POSSIBLE DETECTION OF A JAHNSITE-WHITEITE GROUP PHOSPHATE MINERAL BY MSL CHEMIN IN GLEN TORRIDON, GALE CRATER, MARS. A. H. Treiman¹, R. T. Downs², D. W. Ming³, R. V. Morris³, M. T. Thorpe³, R. M. Hazen⁴, G. W. Downs², E. B. Rampe³, and the CheMin MSL team. ¹Lunar and Planetary Institute, 3600 Bay Area Blvd., Houston TX 77058 (treiman@lpi.usra.edu), ²University of Arizona, Tucson AZ, ³ARES, NASA Johnson Space Center, Houston TX, ⁴Carnegie Institution Washington, DC.

Introduction: The CheMin instrument on the Mars Science Laboratory (MSL) Curiosity rover is an X-ray diffractometer, and can detect minerals more abundant than ~1%, determine unit-cell parameters of minerals and corresponding constraints on their compositions, determine the abundances of minerals, and constrain the abundance(s) of X-ray amorphous material(s) [1-3]. In several recently analyzed samples, CheMin has detected a sharp diffraction peak corresponding to a mineral lattice spacing (i.e., d-spacing) of ~9.22Å, which is distinct from any spacing in common rock-forming minerals. This peak could represent a mixed-layer serpentine-talc phase [4,5], or a hydrous manganese-bearing phosphate mineral of the jahnsite-whiteite group [4-6]. In this abstract, we explore the likelihood and implications of the latter.

Diffraction Data: The CheMin instrument is a transmission powder X-ray diffractometer [1]. It generates an X-ray beam, which is collimated and passes through a sample of vibrating, moving powder. Diffracted X-rays are collected on an energy-dispersive CCD plane, and the results processed to yield typical 1-dimensional XRD patterns (Fig. 1). The 1-D patterns are processed with the software programs JADE[®] and FULLPAT [7] to give diffraction d-spacings, mineral identifications, compositional constraints, and proportions of crystalline and X-ray amorphous materials.

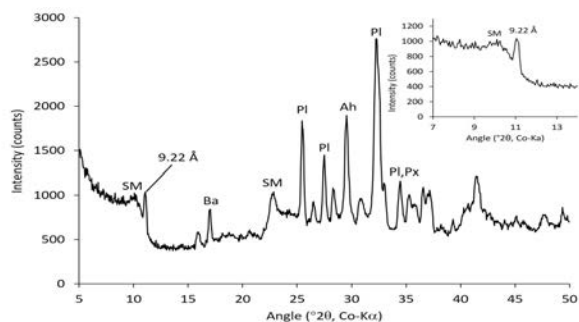


Figure 1. CheMin XRD pattern for the Groken sample (GR). Strongest peaks indicated for: ~9.22Å phase, smectite (SM), plagioclase (PI), pyroxene (Px), anhydrite (Ah), and bassanite (Ba). Inset upper right is a close-up of the area of the ~9.22Å peak

The ~9.22Å diffraction peak (Fig. 1) has been detected only in samples from the Glen Torridon trough, and not earlier in the mission; it does not correspond to any minerals reported earlier. The ~9.22Å peak is as sharp as the instrument permits (Fig. 2), much sharper

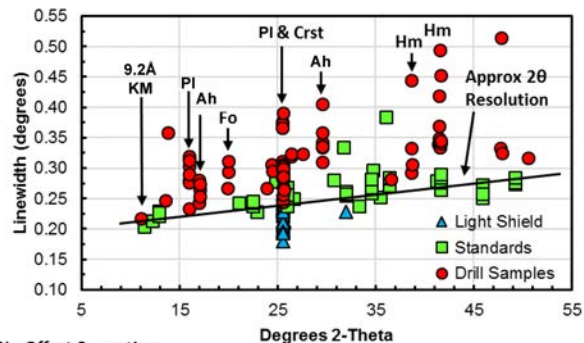


Figure 2. Diffraction peak Full Width - Half Max for CheMin XRD patterns on Mars. The 9.22Å datum is for the Kilmarie (KM) sample; its width is consistent with a highly ordered crystal. (Light Shield is an artifact). Mineral abbreviations as in Fig. 1, plus olivine (Fo), cristobalite (Crst), and hematite (Hm).

than the adjacent smectite diffraction, which implies that the peak comes from a well-crystallized phase.

Geological Setting: The ~9.22Å peak has been detected in several drill samples across the Glen Torridon area, formerly known as the clay-bearing trough (Fig. 3). The rock here is assigned to the Murray formation [5], clay-bearing lacustrine mudstones and sandstones that Curiosity has traversed for many kilometers. The strongest 9.22Å diffractions are in the Kilmarie, Mary_Anning3, and Groken samples (Fig. 1), with smaller but detectable peaks in Aberlady, Mary_Anning, and Glen_Etive (Fig. 3). Groken, a few



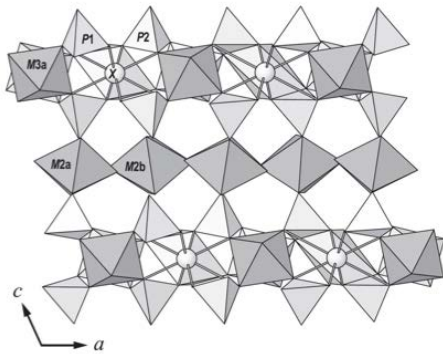
Figure 3. Sample drill locations in the Glen Torridon area, Red circles show detections of the 9.22 Å phase; white circles lack such detection. DU-Duluth; ST-Stoer; HF-Highfield; RH-Rock_Hall; KM-Kilmarie; AL-Aberlady; GE-Glen_Etive; GG-Glasgow; HU-Hutton; EB-Edinburgh; MA-Mary_Anning; GR-Groken.

meters from Mary Anning, was drilled because it contains many dark polygonal objects and is enriched in P and Mn [5,8-10]. These characteristics suggest diagenesis involving Mn, which (by its several valence states) can serve as an energy source for chemosynthetic microorganisms.

Jahnsite-Whiteite Group Minerals: To determine the mineral responsible for the $\sim 9.22\text{\AA}$ diffraction peak, the CheMin team searched diffraction databases (ICDD, AMCSDB [11]) for substances that: have a strong diffraction peak at $\sim 9.22\text{\AA}$, contain only abundant rock-forming elements (and Zn [12]), have no diffraction peaks inconsistent with observed patterns (Fig. 1), and have other diffraction peaks that help account for otherwise unexplained intensities in the observed XRD patterns.

These criteria are best fit by minerals of the jahnsite-whiteite group [6]. These are hydrous phosphates, with alternating layers of PO_4 tetrahedra and layers of metal cations in 6- or 8-fold coordination with oxygens (Fig. 4) [6,13]. Their crystal structure supports extensive solid solutions: in their octahedral M3 sites, jahnsites have Fe^{3+} dominant while whiteites have Al^{3+} dominant (Fig. 4). The octahedral M1 & M2 sites typically contain Fe^{2+} , Mg, Mn^{2+} , and/or Fe^{3+} ; the X site is an 8-fold coordinated cage of oxygens that can hold Ca, Na and/or Mn^{2+} . The group's nomenclature [name - (X M1 M2)] reflects this extensive variability, e.g.:

whiteite-(MnMnMg) = $\text{MnMnMg}_2\text{Al}_2(\text{PO}_4)_4(\text{OH})_2 \cdot 8\text{H}_2\text{O}$;
jahnsite-(CaFeMg) = $\text{CaFe}^{2+}\text{Mg}_2\text{Fe}^{3+}_2(\text{PO}_4)_4(\text{OH})_2 \cdot 8\text{H}_2\text{O}$.



The crystal structure of whiteite-(MnMnMg) viewed along [010].

Figure 4. Whiteite's atomic arrangement [13], viewed parallel to its layers, i.e., perpendicular to (001). P1 & P2 are PO_4^{3-} tetrahedra. M3 are octahedral sites that hold Al^{3+} and/or Fe^{3+} . Octahedral sites M2 & M1 (not visible) hold small divalent cations (Mg, Mn^{2+} , Fe^{2+} , Zn). The 8-fold X site can hold Ca, Na, or Mn^{2+} .

Paragenesis: Minerals of the jahnsite-whiteite group have not been reported on Mars or from meteorites [14], and are widely distributed although volumetrically minor on Earth. Most reports are from granitic pegmatites (e.g., [15-17]) as alterations of primary Fe and/or Mn phosphates, and commonly associated with:

hereaulite, $\text{Mn}^{2+}_5(\text{PO}_3\text{OH})_2(\text{PO}_4)_2 \cdot 4\text{H}_2\text{O}$; vivianite, $(\text{Fe}^{2+}\text{Fe}^{2+}_2)(\text{PO}_4)_2 \cdot 8\text{H}_2\text{O}$; and rockbridgeite, $(\text{Fe}^{2+}, \text{Mn})(\text{Fe}^{3+})_4(\text{PO}_4)_3(\text{OH})_5$. Minerals of the jahnsite-whiteite group occur in many other environments: altered phosphatic iron formations (e.g.: Iron Monarch mine, South Australia [13]; Rapid Creek formation, Yukon, Canada [18,19]); altered shale/chert [20]; oil shale [21]; and urinary stones [22]. The thermochemical stabilities of jahnsite-whiteite group minerals are unknown, although they dehydrate at $\sim 200^\circ\text{C}$ [13,23].

Gale Crater: Given that jahnsite-whiteite minerals are found in a wide range of environments on Earth, it is conceivable that they could also form during diagenesis on Mars. There is ample evidence for diagenesis in the Murray formation mudstones, including mobility and recrystallization of iron oxides on Vera Rubin Ridge [24,25] and formation of Mn-rich nodule in Glen Torridon [5,8-10]. For the environments of Glen Torridon rocks, jahnsite-whiteite group minerals could have formed during low-temperature alteration of apatite by acid sulfate solutions rich in Mn (and possibly Fe). It is not clear why jahnsite-whiteite might be present alone, without detections of any other secondary phosphate minerals.

Acknowledgments: Dr. R.H. Jahns, for whom jahnsite is named, advised the first author's M.S. thesis at Stanford University in 1974-1977.

References: [1] Blake D.F. et al. (2012) *Solar Syst. Res.* 170, 341-399. [2] Rampe E.B. et al. (2020) *Geochem.* 80, 125605. [3] Morrison S. et al. (2018) *Amer. Mineral.* 103, 857-871. [4] Bristow T. et al. (2021) *JGR:Planets*, in preparation. [5] Thorpe M.T. et al. (2021) *LPSC 52*, this volume. [6] Moore P.B. & Ito J. (1978) *Mineral. Mag.* 42, 310-323. [7] Chipera S.J. & Bish D.L. (2002) *J. Appl. Cryst.* 35, 744-749. [8] Berger J. et al. (2021) *LPSC 52*, this volume. [9] Lanza N.L. et al. (2021) *LPSC 52*, this volume. [10] Gasda P.J. et al. (2021) *LPSC 52*, this volume. [11] Downs R.T. & Hall-Wallace M. (2003) *Amer. Mineral.* 88, 247-250. [12] Lasue J. et al. (2016) *JGR:P* 121, 338-352. [13] Elliott P. & Willis A.C. (2019) *Can. Mineral.* 57, 215-223. [14] Rubin A.E. & Ma C. (2020) Meteorite Mineralogy. In *Oxford Research Encyclopedia of Planetary Science*. [15] Moore P.B. & Araki T. (1974) *Amer. Mineral.* 59, 964-973. [16] Kampf A.R. et al. (2018) *Can. Mineral.* 56, 871-882. [17] Grey I.E. et al. (2010) *Mineral. Mag.* 74, 969-978. [18] Robertson B.T. (1982) *Can. Mineral.* 20, 177-187. [19] Robertson B.T. & Young F.G. (1984) 361-371 in *The Mesozoic of Middle North America: A Selection of Papers from the Symposium on the Mesozoic of Middle North America*, AAPG Memoir #9. [20] Kampf A.R. et al. (2016) *Can. Mineral.* 54, 1513-1523. [21] Loughnan F.C. et al. (1983) *Mineral. Mag.* 47, 327-334. [22] Abboud I.A. (2008) *Environmental Geochemistry and Health*, 30(5), 445-463. [23] Grice J.D. et al. (1990) *Amer. Mineral.* 75, 401-404. [24] Achilles C.N. et al. (2020) *JGR:Planets* 125, e2019JE006295. [25] Rampe E.A. et al. (2020) *JGR:Planets* 125, e2019JE006306.